An experimental and theoretical study of martensitic phase transitions in Li and Na under pressure

1989 J. Phys.: Condens. Matter 1 5319

(http://iopscience.iop.org/0953-8984/1/32/001)

J. Phys.: Condens. Matter 1 (1989) 5319–5335. Printed in the UK

An experimental and theoretical study of martensitic phase transitions in Li and Na under pressure

V G Vaks†, M I Katsnelson‡, V G Koreshkov‡, A I Likhtenstein§, O E Parfenov†, V F Skok‖, V A Sukhoparov‖, A V Trefilov† and A A Chernyshov†

† I V Kurchatov Institute of Atomic Energy, Moscow 123182, USSR
‡ Institute of Physics of Metals, Sverdlovsk 620219, USSR
§ Institute of Chemistry, Sverdlovsk 620219, USSR
‖ Institute of High Pressure Physics, Troitsk, Moscow 142092, USSR

Received 31 May 1988

Abstract. By using the methods of acoustic emission and neutron-structure analysis, the effect of pressure p on low-temperature phase transitions in Li and Na is investigated. In Li, within the investigated interval of $p \leqslant 3$ GPa, the transition temperature rises with pressure, and the low-temperature phase has a 9R structure. In Na, on the contrary, pressure suppresses the transition, so that it disappears even at $p = 0.1$–0.2 GPa but the 9R phase is the low-temperature one too. The shape of acoustic emission signals suggests the presence of pre-transition phenomena and differences in the kinetics of transitions in Li and Na. Calculations performed explain the difference in the influence of pressure on structural stability of Li and Na by the effect of proximity of the Fermi level to peaks in the electronic density of states, which appears under pressure in Li but is absent from Na. The same effects account for a pre-martensitic softening of the shear constant, observed under compression of Li.

1. Introduction

Lithium and sodium have a simple electronic structure and seem to be one of the simplest subjects for study of the character and nature of martensitic phase transitions (PT) in metals. With decreasing temperature T, these metals go over from the BCC into close-packed phases of the HCP type or structures close to the latter. These PT found by Barrett (1956) were treated in a great number of experimental and theoretical studies, which are still continuing. Temperatures M_s of the beginning of martensitic PT at atmospheric pressure $p \simeq 0$ equal 70–80 K in Li and 30–35 K in Na (Barrett 1956, Chernyshov *et al* 1983). The pseudopotential calculations (Vaks *et al* 1977b, Young and Ross 1984) predicted a drop of M_s and disappearance of the PT with rising p, in contrast with simple geometrical considerations about increasing stability of close-packed phases with pressure. Experiments (Chernyshov *et al* 1983) confirmed this prediction for Na. However, in Li M_s did not drop under compression but increased, at least, up to $p = 1.7$ GPa. This increase of M_s with p agrees with the structural PT observed in Li at $T = 296$ K, $p = 6.9$ GPa (Olinger and Shaner 1983). Measurements of the electrical

0953-8984/89/325319 + 17 $02.50

resistance $R(p, T)$ in Li also confirmed the increase of M_s with p (Oomi and Woods 1985) and indicated the presence of one more structural PT at low T for $p \simeq 26$ GPa (Lin and Dunn 1986). The data on $R(p, T)$ in the $Li_{0.9}Mg_{0.1}$ alloy also suggest a possible change of the $M_s(p)$ dependence character, i.e. a change-over from increase to decrease, at very small $p \simeq 0.2$ GPa (Oomi *et al* 1987).

The structure of low-temperature phases at $p = 0$ in Li and Na was determined by Barrett (1956) as a HCP one, though it was noted that cold working transformed a HCP Li into a FCC one. Subsequent investigations (McCarthy *et al* 1980, Overhauser 1984, Berliner and Werner 1986, Smith 1987) showed that at $p = 0$ the low-temperature phase of Li had most likely a 9R structure (of the Sm type) with numerous packing defects. At $T = 296$ K, $p \simeq 6.9$ GPa the Li structure was determined by Olinger and Shaner (1983) as FCC. However, this conclusion raises doubts, since the authors observed only two reflections which coincide in the FCC, HCP and 9R phases. Thus, on the whole the form of phase diagrams and structure of Li and Na under pressure have been studied insufficiently so far. This is due to methodological difficulties arising when one handles alkali metals under extreme conditions (high pressures, low temperatures), as well as with very slight variation of macroscopic characteristics at PT and complicated kinetics of martensitic transformations.

Theoretically, stability of Li and Na phases was investigated by using empirical pseudopotentials (Vaks *et al* 1977b, Young and Ross 1984), as well as *ab initio* calculations (McMahan and Moriarty 1983, Skriver 1985, Dacorogna and Cohen 1986, Zdetsis 1986). However, as the structure energy differences ΔE_{ij} in Na and Li are abnormally small, $\Delta E \sim 0.01$–0.1 mRyd/atom (Vaks *et al* 1977b), the accuracy of *ab initio* calculations seems to be insufficient here, and $\Delta E_{ij}(p)$ differs in the above-mentioned calculations both quantitatively and qualitatively. At the same time, the accuracy of the pseudopotential calculations of alkali-metal properties is usually high enough (see e.g. Bratkovsky *et al* 1984 and references therein). Therefore, it seems important for the development of the theory of crystal structure stability in metals to find out the reasons for the above-mentioned qualitative discrepancy between experiment and the $M_s(p)$ dependence predicted by Vaks *et al* (1977b) for Li, while agreement is obtained for Na.

The present work is a continuation of the previous studies (Chernyshov *et al* 1983, Vaks *et al* 1977b) of PT in Li and Na under pressure. In §§ 2 and 3 we describe experiments within intervals of pressure and temperature broader than earlier: up to 3 GPa in Li and under the conditions of purely hydrostatic gas pressure up to 0.25 GPa and T down to 4.2 K in Na. To observe the PT, we used the acoustic emission method, while crystal structures were determined by using the neutron diffraction method. The results obtained make appreciably more accurate and complete the conclusions (Chernyshov *et al* 1983) about phase diagrams, phase structures and PT kinetics. In particular, 9R is a low-temperature structure both for Li (at $p = 0$ and $p = 0.4$ GPa) and for Na.

In §§ 4 and 5 we discuss the electronic theory of PT in Li and Na employing both the pseudopotential and *ab initio* calculations. It is shown that the differences in the $M_s(p)$ dependence for Li and Na are connected with qualitatively different changes in the band structure with pressure. In Li the Fermi level ε_F approaches the ε_c point of the peak in the density of states with rising p (which was not taken into account in the pseudopotential calculations (Vaks *et al* 1977b, Young and Ross 1984)), and the arising band effects (Vaks and Trefilov 1988) result in a drop of the BCC phase stability, thus stimulating a BCC–9R or BCC–FCC PT. For Na these effects of approach of ε_F to ε_c are absent, and, in compliance with Vaks *et al* (1977b) and Young and Ross (1984), the decrease of relative

contribution of the band effects to the energy in compression causes an increase of the BCC phase stability. The above band effects in Li should also result in the 'softening' of shear constants c_s with pressure (Vaks and Trefilov 1988). This agrees with recent experiments (Voronov *et al* 1987) and explains a general character of the 'pre-martensitic' softening of $c_s(p)$, observed in a number of systems (Voronov and Stalgorova 1973, Goncharova *et al* 1982).

2. Experimental method

Two different experimental facilities were used to create high pressures and low temperatures.

Measurements with lithium were performed in 'cylinder–piston' type pressure cells placed in a helium cryostat of flowing-gas type. The pressure was transferred from a hydraulic press through thermo-insulated columns (Vindryaevsky *et al* 1980). The minimum temperature achieved under these conditions amounted to 10 K. The maximum attainable pressure was determined by the design and material of the high-pressure cell. A pressure cell made of aluminium alloy was used to identify the crystal structure of Li by means of neutron diffraction analysis under a pressure up to 0.5 GPa. The sample was 20 mm in diameter and 50 mm in length. A pressure cell made of carboloy was used in the pressure range up to 3 GPa. The sample had the volume about 1 cm^3. The sample was pressed without pressure medium and the pressure was measured to within 5% by the piston-displacement method. The high plasticity of lithium ensured a sufficiently hydrostatic pressure, which was manifested by the width of diffraction peaks in the neutron diffraction pattern. The temperature was measured by a carbon resistance thermometer placed in the channels of the cell body. The temperature gradient along the sample was less than 0.5 K cm^{-1}. To detect the acoustic emission (AE), a piezoceramic transducer glued onto the outer wall of the pressure cell was used. The onset of the phase transformation was detected by an AE peak appearing during a cooling of the sample at a fixed stress on the pressure cell piston.

In Na the phase transition takes place at lower temperatures and pressures than in Li. For its investigation, the second experimental facility was used with a high-pressure gas cell and a helium cryostat allowing operation in the pressure range 0–0.25 GPa and the temperature range 300–1.5 K. The pressure was generated by a diaphragm compressor and transferred to the pressure cell through a capillary. Gaseous helium served as pressure-transfer medium, which ensured a highly hydrostatic pressure. The pressure was measured by a standard pressure gauge to within 1% accuracy. The temperature measurement accuracy taking into account the gradient amounted to 0.2 K. For Na the quantity of new phase formed in cooling is very small (~7% at 5 K (Barrett 1956)), while for Li it amounts to more than 50%. Therefore, to increase the AE method sensitivity, the piezo-transducer was arranged inside the cell in immediate acoustic contact with the sample. For this purpose a vacuum-tight lead into the pressure cell was employed (Sukhoparov and Telepnev 1980).

As has been mentioned above, to detect the phase transformation, we used the AE method, i.e. a phenomenon consisting of radiation of ultrasonic waves in solids, arising due to a change in internal structure accompanied by elastic energy release. In particular, martensitic-type phase transformations are an intensive source of AE in solids. Though the microscopic mechanism of generating such signals has not been directly investigated so far, a number of experimental data allow us to suggest that they arise because of

non-stationary motion of inter-phase boundaries which move with sound velocities at martensitic transformations. In fact, by the AE signals one can observe nucleation of separate martensitic plates, which makes this method much more sensitive than others detecting changes of various physical quantities averaged over the volume of a sample. Moreover, the AE method is convenient technically when operating under high pressures, since acoustic signals pass through a metal wall of the cell rather easily and can be detected by an outer transducer. In principle, the AE signals contain diverse information on the phase transition process but for the given problem it suffices to confine ourselves to measurement of the AE signal count rate on varying the sample thermodynamic parameters. The signals from the transducer were sent to the electronic system, at the output of which one can obtain information on the acoustic radiation power, number of signals and their amplitude distribution.

The phase transformations were studied by using samples of Li and Na with a chemical purity no worse than 99.9%. For the neutron-structure investigations a sample containing 99% of ^{7}Li was used, as natural lithium contains about 7% of ^{6}Li having a large neutron absorption cross section. The measurements were made by a time-of-flight many-detector diffractometer on the linac 'Fakel' at the I V Kurchatov IAE (Vindryaevsky *et al* 1981), which allows up to 16 neutron diffraction patterns to be obtained for different scattering angles, This is significant to identify the structure of coarse-grained polycrystals such as samples of Li and Na usually are.

3. Experimental results

3.1. Phase diagrams

It is possible to initiate a phase transition by changing both temperature and pressure. A major part of the measurements was made by using the first method. In this case the AE background from the cell is much lower and the transition itself is much more distinct, since the lines of the PT start in the p–T diagram close to horizontal. Inasmuch as the martensitic transitions proceed according to athermic kinetics and display a noticeable hysteresis, we can determine four characteristic temperatures: M_s, M_f correspond to the start and finish of the low-temperature martensitic phase formation, and A_s, A_f are the respective temperatures of the inverse transformation into a high-temperature 'austenite' phase.

Figure 1 presents a characteristic form of the AE intensity dependence on temperature at phase transformations in Li and Na. A transition to the martensitic phase in sample cooling is very pronounced, while the emission in heating turns out to be 100–200 times weaker. Therefore, the inverse transition temperature was clearly detected only at $p = 0$. As seen from figure 1, the AE method allows the martensitic transformation to be detected positively enough and M_s to be determined with good accuracy. However, the problem of obtaining unambiguous reproducible results is more complicated. The M_s value is affected appreciably by various kinds of crystal lattice defects, which, as a rule, lower the threshold of new phase nucleation and, consequently, raise M_s. It has been experimentally established that the full annealing of strains due to the phase transformation takes place at $T \gtrsim 250$ K. Therefore, the pressure was always generated at a higher temperature and maintained constant during the whole cooling process.

Note some characteristic features of the AE, which are not directly connected with the study of Li and Na phase diagrams but are, apparently, interesting from the viewpoint

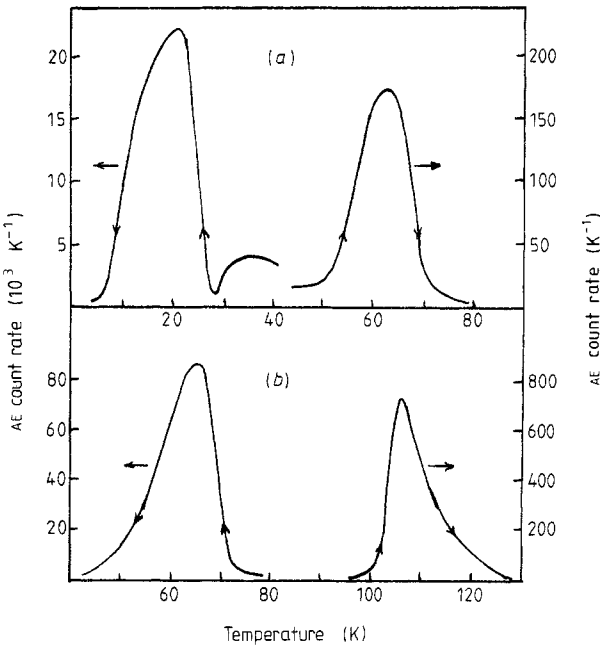

Figure 1. Acoustic emission peaks at the martensitic transformation in (*a*) Na and (*b*) Li in cooling and heating of the sample.

of martensitic transformation kinetics in these metals. As a rule, a range of weaker emission is observed before the AE main peak, which may be due to some pre-transition processes. During the transition itself the emission has an 'explosive' character: there occurs a sharp increase of acoustic signal generating rate at decreasing temperature below M_s. A time correlation of the signal appearance is noticeable, which suggests reaction autocatalysis. By the end of the transformation a gradual decrease of the signal amplitude takes place down to the amplifier noise level at a noticeable increase of their generating rate. The amplitude spectrum measurements have shown that in all cases it displayed the form of a curve increasing to small amplitudes according to a law close to hyperbolic. The noted AE peculiarities underwent no significant change throughout the whole range of pressures investigated, which suggests the same character of the phase transition under these pressures.

The dependence $M_s(p)$ obtained for both metals is given in figures 2 and 3. The appreciable spread of the experimental points exceeds the individual measurement error and is explained by the above-mentioned difficulties due to the martensitic transformation complex kinetics. The transition temperature M_s in Li rises with increasing pressure at an average rate of $dT/dp = 15\ \mathrm{K\ GPa^{-1}}$.

The slope of the phase diagram for Na turns out to be opposite; $M_s(p)$ drops quickly with pressure at the average rate of $dT/dp = -170\ \mathrm{K\ GPa^{-1}}$. Experimental points on the $M_s(p)$ curve are given only to the pressure $p = 0.09$ GPa, as the pressure-transfer helium solidifies at this point and it becomes difficult to control the pressure accurately. Moreover, helium solidification may initiate the PT in sodium. The arrows in figure 3 indicate pressures at which no PT was observed in experiments on the sample cooling down to 4.3 K. Thus, for Na the region of low-temperature phase existence narrows quickly with rising pressure and at high pressures the BCC phase turns out to be stable at all temperatures. This conclusion following from the preliminary results given by

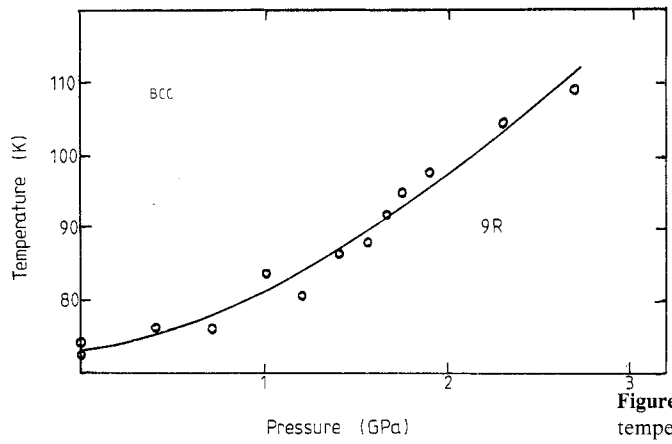

Figure 2. The martensitic transformation temperature M_s versus pressure in Li.

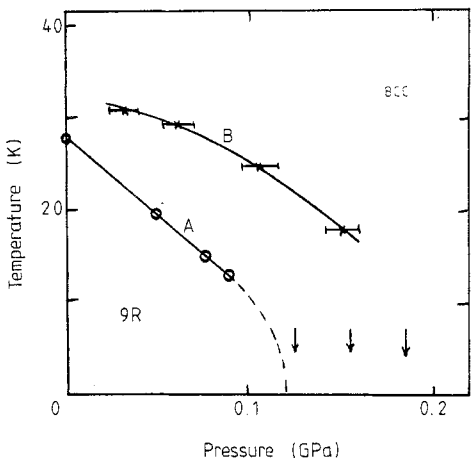

Figure 3. The martensitic transformation temperature M_s versus pressure in Na: A, the beginning of transformation, M_s, in cooling p = const; B, the beginning of transformation for decreasing pressure, T = const.

Chernyshov *et al* (1983) was confirmed, though the $M_s(p)$ values obtained at gas pressures turned out to be somewhat lower. Such a deviation may be accounted for by the incompletely hydrostatic pressure in the 'cylinder–piston' pressure cell. Inhomogeneity of strains creates conditions for the start of transformation at smaller overcooling.

It is known (Barrett 1956) that by cold mechanical working of the sample one succeeds in bringing the temperature of the PT onset to the thermodynamic phase equilibrium point M_d. One may expect that in our case the pressure change will result in the same effect because of unavoidable shear stresses in the sample under pressure. To this aim, the measurements with sodium were also made under pressure-changing conditions at a fixed temperature. Indeed, in this case with decreasing pressure the martensitic transition started earlier, as shown by curve B in figure 3. It is important that the slope of this curve is also negative; thus, the conclusion is confirmed about the increase of the BCC phase stability with rising pressure predicted by Vaks *et al* (1977b) and McMahan and Moriarty (1983).

3.2. Structural investigations

Our first neutron diffraction studies performed on lithium at normal pressure and temperature of 60 K revealed the existence of clear reflections in the neutron diffraction

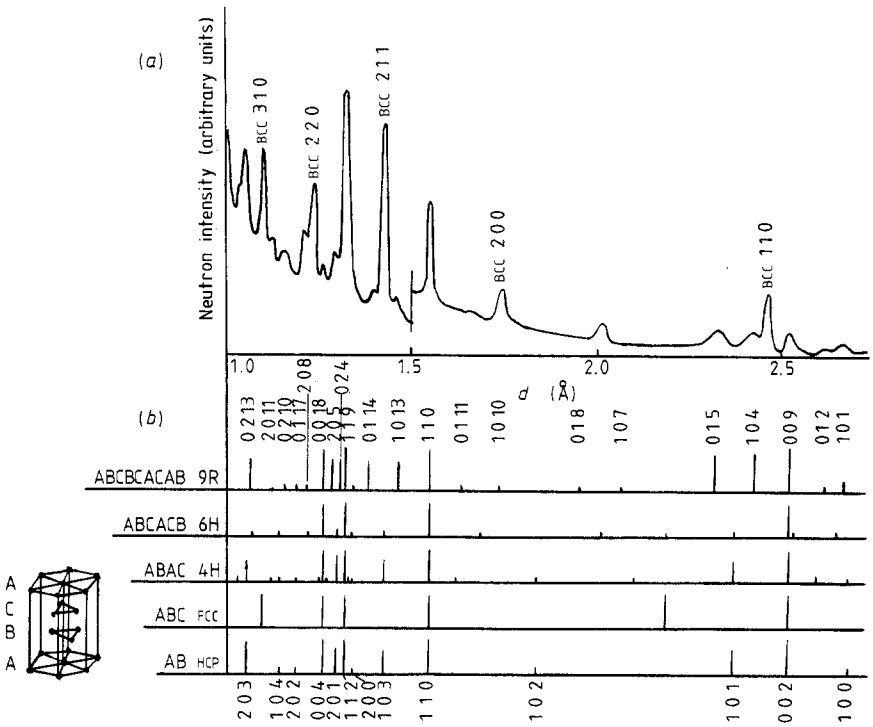

Figure 4. The structure of a low-temperature phase for Li: (*a*) a fragment of the experimental neutron diffraction pattern (^{7}Li, $T = 60$ K, $p = 0$); (*b*) neutron-structure factors calculated for different packings of hexagonal layers.

pattern, which we attributed to 1 1 0 and 1 1 2 of the HCP structure. Hence, the values of the parameters were found: $a = 3.096$ Å and $c = 5.038$ Å (Chernyshov *et al* 1983). Simultaneously, a number of weaker reflections were observed, not all of which could be related to the HCP structure. On the basis of analogous neutron data (McCarthy *et al* 1980), Overhauser (1984) discussed the possibility of a more complicated packing of hexagonal layers, using which a number of more long-period structures could be constructed (besides the HCP and FCC lattices) of the type 4H (double HCP), 6H (triple HCP) and 9R, realised in some rare-earth metals (Skriver 1985).

Figure 4 presents a fragment of our neutron diffraction pattern and shows the positions of possible reflections for all the above-mentioned types of packing. It is clear that the positions of the most intensive reflections of the *hhl* type, which were used to determine the lattice parameters, coincide for all the structures. The differences are due to weaker reflections, the number of which increases with increasing packing period. The data given in figure 4 and a more detailed analysis of all the neutron diffraction patterns show that the 9R structure is most probable. However, this structure does not display complete coincidence in the position and number of observed reflections either. Stacking faults (Berliner and Werner 1986), as well as admixture of the phase with the 6H structure (a reflection at $d = 2.01$ Å), might be possible reasons for the discrepancies observed.

In order to interpret the lithium phase diagram with confidence, it was necessary to perform structural measurements at high pressures as well. Such measurements were

made at $p = 0.4$ GPa. The basic feature of the low-temperature phase, 9R, remained the same. Though the background from the pressure cell complicates the neutron diffraction pattern analysis, we can nevertheless assert that the 6H phase signs disappeared. It is possible to assume that, as a result of the phase transition, the system finds itself in the metastable state, the properties of which depend appreciably on the conditions of the transition process.

Analogous neutron-structure measurements were made for sodium. However, it was difficult to determine the low-temperature structure unambiguously in the process of cooling at a constant pressure because the concentration of the martensitic phase obtained was very low. It was only as a result of a cyclic variation of pressure in the low-temperature region that we succeeded in the resolution of several of the strongest reflections of the martensitic phase. The low-temperature phase of Na turns out to have the 9R structure, as is the case for Li (in contrast with the determination of Barrett (1956)). The noticeable shifts of some diffraction peaks, in particular, of the 015 one, indicate the presence of a number of stacking faults in the martensitic phase, as was also reported for Li by Berliner and Werner (1986).

Thus, the results of our investigations yield the 9R structure for low-temperature phases in both Li and Na. However, the problem of the degree of perfection for these structures and proximity to equilibrium ones requires further research. Our structural investigations for sodium will be described in more detail elsewhere.

4. Stability of crystal phases and band structure of Li and Na under pressure

In the present section we give the results of calculating the energy differences and those for the band structure in different Li and Na phases. Attention will be paid mostly to qualitative discussion of the connection between stability and band structure. For this purpose it suffices to consider the case of zero temperatures $T = 0$. Thus the form of phase diagrams (p, T) for $T \neq 0$ will be evident qualitatively, and they can be calculated quantitatively in the same way as was done by Vaks *et al* (1977b) (hereafter referred to as I).

Under pressure p the stability of the i phase with respect to the j one is determined by the condition $\Delta\Phi_{ij}(p) = \Phi_i - \Phi_j < 0$, where $\Phi_i = E_i + p\Omega_i$ is the Gibbs potential of the i phase (per atom). But since the atomic volumes Ω of the phases considered are close, $\Delta\Omega/\Omega \sim 10^{-3}$ (see I), $\Delta\Phi_{ij}$ is close to the energy difference at a fixed volume, $\Delta E_{ij}(\Omega) = E_i(\Omega) - E_j(\Omega)$: $\Delta E_{ij} - \Delta\Phi_{ij} \simeq \frac{1}{2}B(\Delta\Omega/\Omega)^2$, where B is the bulk modulus. In our calculations this difference does not usually exceed a few per cent of ΔE_{ij}. Therefore, in the present work (as was done by McMahan and Moriarty (1983), Skriver (1985), Dacorogna and Cohen (1986) and Zdetsis (1986)) only $\Delta E_{ij}(\Omega)$ is given for simplicity, while the Ω dependence on the pressure p in figure 5 corresponds to the BCC phase.

4.1. Pseudopotential calculation

In the present calculation we make use of the same second-order pseudopotential model as before (see I, Vaks and Trefilov 1988) but in addition to the BCC, FCC and HCP phases discussed in I we shall also consider the 9R, 4H and 6H structures mentioned in § 3. If we denote, as usual, the sequence of packing of 'hard-sphere' layers in the HCP and FCC phases as ABAB... and ABCABC..., then for 4H, 6H and 9R structures these

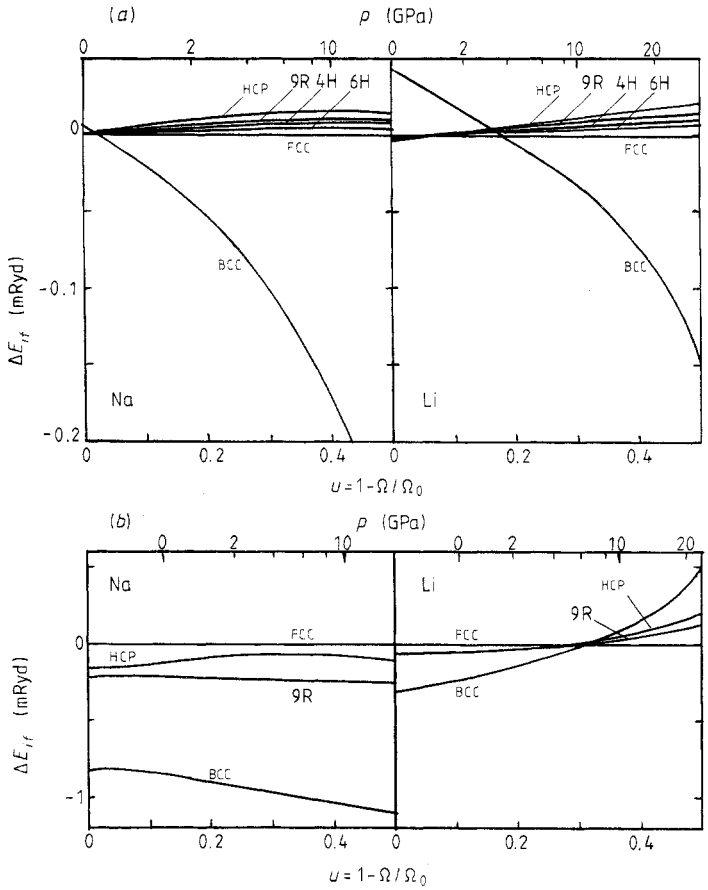

Figure 5. Structure energy differences $\Delta E_{if} = E_i - E_f$ with respect to the FCC phase versus compression u: (*a*) calculation in the frame of the pseudopotential perturbation theory (PPT); (*b*) calculation using the LMTO–ASA method. The ΔE_{if} scale in (*b*) is an order of magnitude lower than that in (*a*). Calculated values of the pressure $p(u)$ are given in the upper parts of the figures.

packings have the form: ABAC. . ., ABCACB. . . and ABCBCACAB. (Overhauser 1984).

In second order in the pseudopotential V the difference of free energies of the phases, $\Delta F_{ij} = F_i(\Omega, T) - F_j(\Omega, T)$, has the form

$$\Delta F_{ij}(\Omega, T) = \Delta E_{ij}^{\mathrm{Mad}}(\Omega) + \Delta E_{ij}^{\mathrm{bs}}(\Omega) + \Delta F_{ij}^{\mathrm{ph}}(\Omega, T). \tag{1}$$

Here E^{Mad}, E^{bs} and F^{ph} stand for the Madelung energy, the band-structure energy and the phonon contribution to F, and are given by the expressions (see e.g. Brovman and Kagan 1974):

$$E_i^{\mathrm{Mad}} = -\alpha_i z^2 e^2 / 2 r_{\mathrm{WS}} \tag{2a}$$

$$E^{\mathrm{bs}} = -\sum_{g} F(g) |S(g)|^2 \qquad F(q) = \tfrac{1}{2}\Omega V^2(q)\, \Pi(q)/[1 + (4\pi e^2/q^2)\Pi(q)] \tag{2b}$$

Table 1. Values of the Madelung constants α_i in equation (2*a*).

Phase	BCC	FCC	6H	4H	9R	HCP
$10^4(1.792-\alpha_i)$	1.41	2.53	2.77	2.88	3.00	3.24

Table 2. Differences of zero vibration energies, ΔE_{ij}^{zp} (in mRyd), at $\Omega = \Omega_0$ (Vaks *et al* 1977b).

Phases	FCC–BCC	HCP–FCC	Ω_0 (au)
Li	0.0321	0.0011	143.4
Na	0.0131	0.0004	254.5

$$F^{ph} = E^{zp} + \frac{1}{N}T\sum_k \ln\left[1-\exp\left(\frac{-\hbar\omega_k}{T}\right)\right] \qquad E^{zp} = \frac{1}{2N}\sum_k \hbar\omega_k. \tag{2c}$$

In equations (2*a–c*) $r_{WS} = (3\Omega/4\pi)^{1/3}$ is the Wigner–Seitz radius, α_i is the Madelung constant, $\boldsymbol{g}$ denotes the reciprocal lattice vectors, $S(\boldsymbol{g})$ is the elementary cell structure factor, $\Pi(q)$ is a polarisation operator, N is the total number of atoms and ω_k stands for phonon frequencies. Consider the sign and magnitude of each of the three contributions to equation (1).

In table 1 we present the values of the Madelung constants α_i. For hexagonal phases they were calculated at ideal values of the relation $\gamma = c/a$, since γ in the hexagonal phases of Li and Na is close to ideal. If we correlate the indices i = b, f and h with the BCC, FCC and HCP phases, then, according to table 1, the α_i values satisfy the inequalities:

$$\alpha_b > \alpha_f > \alpha_{6H} > \alpha_{4H} > \alpha_{9R} > \alpha_h \tag{3}$$

and the differences $\Delta\alpha_{ij}$ of the neighbouring α_i in the sequence (3) relate to each other, approximately, as 9:2:1:1:2. The relative proximity of α_i in the close-packed (CP) phases reflects geometrical similarity of these phases, and a noticeably higher α_b value is due to the fact that for the BCC phase the Wigner–Seitz cell is closer to a sphere (having the maximum $\alpha = 1.8$) than it is for the CP phases.

The phonon contributions F^{ph} decrease with decreasing frequencies ω_k. Thus, at $T = 0$, $F^{ph} = E^{zp} = \frac{3}{2}\hbar\bar{\omega}_0$; and at high T, $F^{ph} = -3T\ln(T/\hbar\bar{\omega}_h)$, where $\bar{\omega}_0$ and $\bar{\omega}_h$ denote the arithmetic and geometric mean values of the ω_k frequencies. In the phonon spectra of BCC non-transition metals (in particular, alkali metals) there are soft phonon branches Σ_4 (see e.g. Smith 1987), which gives rise to increasing thermodynamic preference of the BCC phase for these metals with increasing T (Zener 1947). The values of the ΔE_{ij}^{zp} differences for the BCC, FCC and HCP phases of Li and Na at equilibrium volume $\Omega_0 = \Omega(T=0)$, calculated in I, are given in table 2. It is clear that the signs of the calculated ΔE_{ij}^{zp} turn out to be the same as those for ΔE_{ij}^{Mad} and that ΔE_{ij}^{zp} between the CP phases are rather small. Comparison of table 2 with figure 5 shows also that the ΔE_{ij}^{zp} contribution to equation (1) is important only at small compressions $u = 1 - \Omega/\Omega_0$. Therefore, in the calculations discussed below for $\Delta E_{ij}^{zp}(u)$ we used simple estimates. $\Delta E_{ij}^{zp}(u) = \Delta E_{ij}^{zp}(0)E_b^{zp}(u)/E_b^{zp}(0)$, and ΔE_{ij}^{zp} between the CP phases was estimated, for definiteness, as $\Delta E_{ij}^{zp} = \Delta E_{fh}^{zp}\Delta\alpha_{ij}/\Delta\alpha_{fh}$, where $\Delta\alpha_{ij} = \alpha_i - \alpha_j$ is the α_i difference from table 1.

The sign of the ΔE_{bi}^{bs} contribution to (1) between the BCC and CP phases turns out to be opposite to that of ΔE_{bi}^{Mad} and ΔE_{bi}^{zp}. This is due to the increase of the function $F(g)$ in (2*b*) in transition from the BCC to the CP structures; see figures 1 and 2 by Vaks *et al* (1977c). In Li and Na it results in the CP phases being energetically favourable at $T = u = 0$ (see I and figure 5(*a*)). However, with increasing compression the ratio $R_i^{bM} = E_i^{bs}/E_i^{Mad}$ in the frame of the considered pseudopotential perturbation theory (PPT) is, generally, dropping. Indeed, the pseudopotential $V(r)$ is a Coulomb interaction of an electron with an ion, being somehow 'truncated' close to the ion core. Therefore, according to the dimensional estimate, R^{bM} is of the order of $ze^2/\hbar v_F$, where v_F is the Fermi velocity, i.e. R^{bM} changes with the volume Ω approximately as $\Omega^{1/3}$. Hence, if the specific 'band' effects of the ε_F proximity to the singular points of the band structure are absent (which is assumed, precisely, in the discussed PPT calculation for univalent metals), the part played by the ΔE^{bs} in equation (1) should decrease with increasing compression, and at sufficiently large u the relative order of the energetic favourability of phases should coincide with the order of the α_i constants in the inequalities (3). These considerations explain the character of the dependences $\Delta E_{ij}(u) = \Delta F_{ij}(u, T = 0)$ in figure 5(*a*), as well as the (p, T) phase diagram form for Na and Li, calculated in I.

As has been noted above, for Na this conclusion about the rise of the BCC phase stability under pressure is confirmed by the experiment; see figure 3. However, for a quantitative calculation of the phase equilibrium temperatures, M_d, the calculation accuracy turns out to be insufficient, which is due to the extreme smallness of the ΔE_{ij} values in Na. According to I, $\Delta E_{bh} \simeq 0.016$ mRyd = 16 μRyd corresponds to the value $M_d \simeq 50$ K (Barrett 1956) observed at $u = 0$, while in I $\Delta E_{bh} = 1.5$ μRyd, $E_{hf} = 1.1$ μRyd were obtained, and in the present calculation (performed in the framework of the same model as in I but to better numerical accuracy) $\Delta E_{bh} = 5$ μRyd, $\Delta E_{hf} = 0.5$ μRyd. However, if we correct the calculation by adding a u-independent constant to $\Delta E_{bh}(u)$, the phase diagram of the BCC–HCP transition in Na is well described by the model used (see I, Chernyshov *et al* 1983, and figure 3) while the difference E_{9R-h} is, evidently, within the accuracy of calculations.

For Li, at $u = 0$, ΔE_{ij} values calculated in the PPT frame are not bad at describing the observed $M_d \simeq 105$ K (see I). Thus it was obtained in I that $\Delta E_{bh} = 41$, $\Delta E_{fh} = 3$, while in the present calculation $\Delta E_{bh} = 37$, $\Delta E_{fh} = 4$, $E_{9R-h} = 1.4$ μRyd (the latter is again within the accuracy of calculations, while in the experiment it is $\Delta E_{9R-h} < 0$). However, the basic qualitative conclusion about the increasing stability of the BCC phase with compression, obtained in the PPT, turns out to be wrong; see figure 2. As discussed below, this is apparently due to the fact that in compression of Li (unlike Na) band effects appear due to Fermi level proximity to a singular point (a peak) in the density of states, which are not taken into account in the conventional PPT (Vaks and Trefilov 1988). We shall treat these effects using the full band calculations.

4.2. Band calculations

The electronic structure of Li and Na was calculated using the self-consistent linear muffin-tin orbitals (LMTO) method in the atomic sphere approximation (ASA) (Andersen 1975, Skriver 1983, Gunnarsson *et al* 1983). The exchange–correlation effects were taken into account by using the Barth–Hedin local potential (Barth and Hedin 1972). The 1s and 1s, 2s, 2p states, respectively, were included into a 'frozen core' in Li and Na, and the 2s, 2p, 3d and 3s, 3p, 3d states, respectively, into the basis of valence orbitals. The calculations were made for the four structures: BCC, FCC, HCP and 9R. The latter was

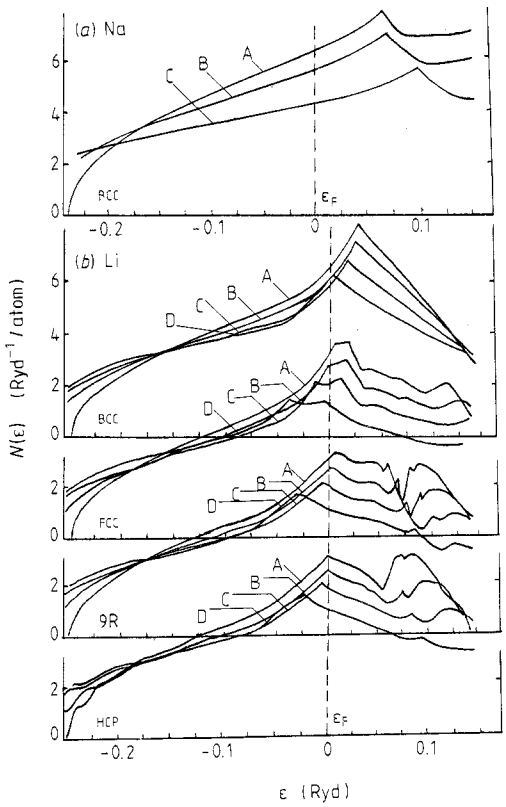

Figure 6. The density of electronic states, $N(\varepsilon)$, in different phases: (*a*) Na; (*b*) Li. The ε values are counted off from the Fermi level ε_F on the abscissa. Curves A, B and C for Na correspond to the compressions $u = 0, 0.2$ and 0.5; curves A, B, C and D for Li correspond to $u = 0, 0.2, 0.4$ and 0.6, respectively.

considered in a trigonal lattice with three atoms in an elementary cell (Wilson and de Podesta 1986) with the parameters taken from Smith (1987). In performing numerical integration over $\boldsymbol{k}$, we sampled the Brillouin zone (BZ) on a mesh of 140, 95, 112 and 140 $\boldsymbol{k}$-points in the irreducible wedge of the BZ for the BCC, FCC, HCP and 9R structures, respectively.

In each structure the total energy E_i was calculated by using the density-functional method with account taken of only the spherical part of the charge density in atomic spheres (Andersen 1975, Skriver 1983), and the pressure p was calculated according to the Pettifor formula (Pettifor 1977). The computation accuracy for the self-consistent calculations used for E was of the order of $10^{-3}\%$, and for p, of the order of 1%. The energy and pressure of zero vibrations were considered to be the same as those in § 4.1 above.

Comparing our and other LMTO calculations for Na and Li (McMahan and Moriarty 1983, Skriver 1985), note that we did not take into account the effects of 'non-rigidity' of 2s and 2p electrons in Na (which could be important at high compressions) and the so-called Madelung and 'combined' corrections to the LMTO–ASA method but, unlike McMahan and Moriarty (1983) and Skriver (1985), we made no use of the 'local-force theorem' for ΔE_{ij} either, i.e. we performed a fully self-consistent calculation of E_i in each of the structures. The band calculation experience available shows that for the density of electronic states, $N(\varepsilon)$, the accuracy of all the LMTO approximations is, usually, high enough. In particular, $N(\varepsilon)$ values calculated by us in the BCC structure of Na and Li at $p = 0$ (figure 6) are close to those obtained in the 'standard' calculations by Moruzzi

et al (1978), where no atomic sphere approximations and linearisation of equations in energy were employed. The errors in the ΔE_{ij} differences in the band calculations usually turn out to be no less than 0.1–1 mRyd (see e.g. Dacorogna and Cohen 1986, Xu *et al* 1987). As seen from figure 5, this does not allow ΔE_{ij} to be calculated quantitatively in Na and Li, which is illustrated by the above-mentioned spread of these values in the calculations (McMahan and Moriarty 1983, Skriver 1985, Dacorogna and Cohen 1986, Zdetsis 1986) as well. However, the accuracy of the LMTO–ASA version used is, evidently, sufficient for determining the qualitative character of the $N(\varepsilon)$ and ΔE_{ij} variations with compression. This is confirmed, in particular, by its successful application to the description of structural PT in other systems (Xu *et al* 1987), as well as by the comparison (see below) of our results with more thorough LMTO calculations (Skriver 1985).

The calculated dependences of the state density $N(\varepsilon)$ on the compression u are given in figure 6. It is clear that for Na and Li these dependences turn out to be qualitatively different. In the BCC Na the distance $\Delta_{cF} = \varepsilon_c - \varepsilon_F$ from ε_F to the singular point (the peak) ε_c in $N(\varepsilon)$ is noticeably larger than that in Li (though in the free-electron approximation it would be $\Delta_{cF}(\mathrm{Li}) \simeq 1.5\ \Delta_{cF}(\mathrm{Na})$, and Δ_{cF} increases with rising u, i.e. ε_c is shifted to the right of ε_F. The same is also true for the FCC, HCP and 9R phases of Na. In Li ε_c is shifted to the left of ε_F under compression, and in the BCC phase there occurs a 'creep-over' of ε_F on the $N(\varepsilon)$ peak. As noted by Vaks *et al* (1988), there appear non-analytical 'band' contributions to the energy, which at small Δ_{cF} cause the increase of E^{bs}; see figure 1(*a*) in Vaks and Trefilov (1988). At the same time in the CP phases of Li the peaks are shifted to the left of ε_F with rising u, which corresponds to the 'overflow' of the Fermi surface over the BZ face and the energy decrease (Vaks and Trefilov 1988). These band effects (which were not taken into account in the above calculations according to the perturbation theory) explain the increase of the BCC phase energy with respect to the CP one in compression of Li in figure 5(*b*). In contrast, in Na, where there are no such band effects, the character of the ΔE_{bi} variation with u turns out to be similar in the LMTO and PPT calculations.

The difference in the dependences $\Delta_{cF} = \varepsilon_c - \varepsilon_F$ for Li and Na is, apparently, due to that in the electron–ion interaction. In Na it is much weaker than in Li (Heine and Weaire 1970), and Δ_{cF} changes with u in the first approximation in the same way as for free electrons: $\Delta_{cF} \sim (\Omega_0/\Omega)^{2/3}$. Otherwise, in Li the interaction in the p state displays a strong resonance-like character, while the states corresponding to ε_c (e.g. in the BCC phase where ε_c corresponds to the point N in the BZ) are 'bonding' states of p type (Heine and Weaire 1970). Therefore, with rising compression ε_c increases much slower than ε_F and Δ_{cF} decreases.

Let us compare our results with other band calculations of ΔE_{ij} in Li and Na. The $\Delta E_{bf}(u)$ and $\Delta E_{hf}(u)$ dependences in figure 5(*b*) are qualitatively similar (for Na, at $u \leqslant 0.3$) to those obtained in the frame of the most thorough LMTO calculation by Skriver (1985). However, in the band calculation with the *ab initio* pseudopotential (Dacorogna and Cohen 1986) the ΔE_{bf} and ΔE_{bh} values in Li decrease with u, at least up to $u \simeq 0.2$. If the energies of the 9R phase observed in Li and of other CP phases are close (which follows from all the calculations presented in figure 5, as well as from the geometrical considerations), the result of Dacorogna and Cohen (1986) disagrees, evidently, with the form of the experimental phase diagram for Li in figure 2. Besides, the ΔE_{bh} values calculated by Dacorogna and Cohen (1986) exceed those estimated above from experimental M_d by 10–15 times. Therefore, the accuracy of the methods used by Dacorogna and Cohen (1986) is, apparently, insufficient for the $\Delta E(u)$ calculations in Li and Na. The results of the cluster band calculation of $\Delta E(u)$ in Li (Zdetsis 1986)

disagree both with ours and with those obtained by Skriver (1985) and Dacorogna and Cohen (1986).

On the whole, the results described in the present section, together with the experimental data given in figures 2 and 3, allow us to assume that at the martensitic PT in Li under pressure the band effects of the structural stability decrease, due to ε_F approaching the $N(\varepsilon)$ peak, manifest themselves clearly. Earlier these effects were discussed for Cs under pressure (Skriver 1985) and for NiTi based alloys (Anisimov *et al* 1987). Below we shall discuss one more manifestation of these effects in Li.

5. 'Pre-martensitic' softening of shear constant in Li under pressure

It has been found in measurements of sound velocities in polycrystal Li at $T = 295$ K and pressures up to 2 GPa (Voronov *et al* 1987) that the shear constant c_s increases with p much slower than the bulk modulus B or than c_s in common metals, e.g. in Na (Vaks *et al* 1978). The extrapolation of the data (Voronov *et al* 1987) to high p allows us to assume that with p further approaching the martensitic PT pressure $p_c \simeq 7$ GPa the softening of c_s will increase and close to p_c it will go over into the decrease of c_s with rising p, as observed in analogous experiments in Ba (Voronov and Stalgorova 1973) and Sr (Goncharova *et al* 1982). Such a softening of c_s is, apparently, another manifestation of the above-mentioned band effects. As discussed by Vaks and Trefilov (1988), this 'band' softening of c_s occurring when ε_F approaches the peak in $N(\varepsilon)$ in the BCC phase of the non-transition metals should be rather pronounced, in particular, for the constant $c' = \frac{1}{2}(c_{11} - c_{12})$. Vaks and Trefilov (1988) illustrated it by using model calculations for $Li_{1-x}Mg_x$ alloys. Here we estimate the $c_s(u)$ dependences in Li and Na employing the same band calculations as in § 4.2.

In order to discuss the given effects in the elastic constants c_{ij}, it is convenient to single out the single-particle 'band' contribution E_b from the energy E, having written E and $c_{ij} = \partial^2 E/\partial u_i \partial u_j$ in the form (Ohta and Shimizu 1983):

$$E = E_{es} + E_b = E_{es} + \sum_\lambda \varepsilon_\lambda \theta(\varepsilon_F - \varepsilon_\lambda) \tag{4a}$$

$$c_{ij} = c_{ij}^{es} + c_{ij}^{b} \qquad c_{ij}^{es} = \partial^2 E_{es}/\partial u_i \partial u_j \qquad c_{ij}^{b} = c_{ij}^{bv} + c_{ij}^{bs} \tag{4b}$$

$$c_{ij}^{bv} = \sum_\lambda \frac{\partial^2 \varepsilon_\lambda}{\partial u_i \partial u_j} \theta(\varepsilon_F - \varepsilon_\lambda) \qquad c_{ij}^{bs} = -\sum_\lambda \frac{\partial \varepsilon_\lambda}{\partial u_i} \frac{\partial \varepsilon_\lambda}{\partial u_j} \delta(\varepsilon_\lambda - \varepsilon_F). \tag{4c}$$

Here u_i denotes the components of the strain tensor, $\theta(x) = 1$ at $x > 0$ and $\theta(x) = 0$ at $x < 0$, E_{es} is the 'electrostatic' energy (being equal to the difference between the Madelung term E^{Mad} and the terms of the electron–electron interaction, E_{ee}, which were counted twice in E_b and ε_λ are the electron energy levels in the self-consistent potential.

It is clear from equations (4*c*) that in the vicinity of the singular point ε_c of the density of states, $N(\varepsilon)$, i.e. at small $\eta = \varepsilon_F - \varepsilon_c$, the function c_{ij}^{bs} has a singularity of the same type as $N(\eta)$ (Vaks and Trefilov 1988), and in c_{ij}^{bv} this singularity is weaker by the degree η. If we suppose that the 'electrostatic' contribution of c_{ij}^{es} at small η also varies more smoothly than c_{ij}^{bs} or than the total c_{ij}^{b}, then it would be possible to use the formulae (4*b*, *c*) for estimation of the band effects in the elastic constants (Ohta and Shimizu

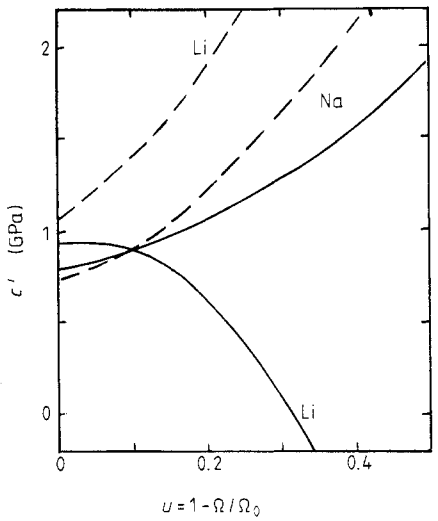

Figure 7. The shear constant $c' = \frac{1}{2}(c_{11} - c_{12})$ in the BCC phase of Li and Na versus u. The broken curves correspond to the calculation in the pseudopotential perturbation theory (Vaks *et al* 1977a); the full curves are the band calculation using our formulae (4) and (5).

1983). For definiteness, in these estimates we shall assume that under compression c_{ij}^{es} changes proportionally to the Madelung contribution:

$$c_{ij}^{es} = A_{ij} c_{ij}^{Mad}(\Omega) \qquad c_{ij}^{Mad}(\Omega) = \beta_{ij} z^2 e^2 \Omega^{-4/3}. \tag{5}$$

The constants β_{ij} in (5) depend only on the lattice type. Thus, in the BCC phase $\beta_{44} = 0.2946$, and for the constant c', $\beta' = 0.0396$. The A_{ij} constants in (5) can be estimated, for example, from the fitting of the constants c_{ij}, calculated according to (4*b*, *c*), to their experimental values at $u = 0$. The A_{ij} obtained for Li and Na turn out to be rather close in value to $A_{ij}^0 = A = \frac{5}{3}$. As will be shown elsewhere, such A corresponds to the model of purely electrostatic interaction E_{ee} of valence electrons of fixed density, which could also be quantitatively reasonable for the simple metals under consideration.

Thus, we estimate the $c_s(u)$ dependences in Li and Na by the formulae (4), (5), assuming $A_{ij} = \frac{5}{3}$. The c_{ij}^b values in (4) were calculated by the method suggested by Ohta and Shimizu (1983). The derivatives of ε_λ with respect to u_i in (4*c*) were found by numerical differentiation over five points in a distorted tetragonal (for c_{44}) or trigonal (for c') lattice with a step in the tetragonality parameter c/a of 1%. Thus the BCC structure itself is represented, correspondingly, as a BCC structure with $c/a = 1$ or a trigonal one with $c/a = 6^{1/2}/4$.

Since the effects considered manifest themselves most strongly in the constant c', we shall discuss the $c'(u)$ dependence in more detail. The results of calculations by formulae (4), (5) are given in figure 7. For comparison, we also present $c'(u)$ values calculated according to the PPT (Vaks *et al* 1977a), used in § 4.1 (for Na they are in good agreement with the data on $c'(u)$ at $u \leqslant 0.1$; Vaks *et al* 1978). One can see that for Na the $c'(u)$ dependences in the PPT and band calculation turn out to be similar, and the same holds for $c_{44}(u)$. For Li the results of the band and perturbation theory calculations again (as in figures 5(*a*) and (*b*)) differ qualitatively: in the band calculation the effects of $c'(u)$ softening with ε_F approaching the $N(\varepsilon)$ peak, discussed by Vaks and Trefilov (1988), manifest themselves clearly. So, in the given estimate the point of the BCC phase instability $c'(u) = 0$ turns out to be close to that of the sign change of the ΔE_{b-9R} difference in figure 5(*b*).

In the constant $c_{44}(u)$ calculated according to (4) for Li (as well as in $c_{44}(x)$ in figure 3 of Vaks and Trefilov (1988)) these effects of softening are much weaker, though at low $\Delta_{cF} = \varepsilon_c - \varepsilon_F$ they are also noticeable. Since the shear constant in a polycrystal is a certain mean value between c' and c_{44}, the presented results of the band calculations of $c_s(u)$ in Li agree qualitatively with the data discussed (Voronov *et al* 1987). Separate measurements of $c'(u)$ and $c_{44}(u)$, i.e. experiments on monocrystals, are evidently desirable for a more detailed check of the theory. The effects of the shear constant band softening under pressure (Voronov *et al* 1987, Voronov and Stalgorova 1973, Goncharova *et al* 1982) will be discussed in more detail elsewhere.

6. Conclusions

The main experimental results of this work are the determination of the 9R structure for the low-temperature phase of sodium and the verification and more exact definition of the earlier (Chernyshov *et al* 1983) conclusion that the effect of pressure on the structural stability of phases in Li and Na is opposite, in spite of the similarity of all the properties of these metals under normal pressures. As shown in §§ 4 and 5, this difference can be explained by the proximity effect of the Fermi level to singular points of the band structure, which appears under pressure in Li but is absent from Na. The considered 'electronic' mechanism of the PT itself, as well as of the pre-martensitic softening of the shear constants, is closely connected with the known considerations of Hume–Rothery–Jones about the phase stability (Heine and Weaire 1970) and can be rather general for structural PT in metals and alloys. Further investigation of these PT, employing relatively simple Li and Li–Mg systems, may be very useful for understanding the nature and peculiarities of such PT.

Acknowledgment

The authors are grateful to G V Peschanskikh for his help in performing the band calculations of the elastic constants $c_{ij}(u)$.

References

Andersen O K 1975 *Phys. Rev.* B **12** 3060
Anisimov V I, Katsnelson M I, Likhtenstein A I and Trefilov A V 1987 *Pis. Zh. Eksp. Teor. Fiz.* **45** 285
Barrett C S 1956 *Acta Crystallogr.* **9** 671
Barth U and Hedin L 1972 *J. Phys. C: Solid State Phys.* **5** 1629
Berliner R and Werner S A 1986 *Physica* B **136** 481
Bratkovsky A M, Vaks V G and Trefilov A V 1984 *Zh. Eksp. Teor. Fiz.* **86** 2141
Brovman E G and Kagan Yu M 1974 *Usp. Fiz. Nauk* **112** 369
Chernyshov A A, Sukhoparov V A and Sadykov R A 1983 *Pis. Zh. Eksp. Teor. Fiz.* **37** 345
Dacorogna M M and Cohen M L 1986 *Phys. Rev.* B **34** 4996
Goncharova V A, Ilyina G G and Voronov F F 1982 *Fiz. Tverd. Tela* **24** 1849
Gunnarsson O, Jepsen O and Andersen O K 1983 *Phys. Rev.* B **27** 7144
Heine V and Weaire D 1970 *Solid State Phys.* **24** 249 (New York: Academic)
Lin T H and Dunn K J 1986 *Phys. Rev.* B **33** 807
McCarthy C M, Tompson C W and Werner S A 1980 *Phys. Rev.* B **22** 574
McMahan A K and Moriarty J A 1983 *Phys. Rev.* B **27** 3235

Moruzzi V L, Janak J F and Williams A R 1978 *Calculated Electron Properties of Metals* (New York: Pergamon)
Ohta Y and Shimizu M 1983 *J. Phys. F: Met. Phys.* **13** 761
Olinger B and Shaner J W 1983 *Science* **219** 1071
Oomi G, Mohammed M A K and Woods S B 1987 *Solid State Commun.* **62** 141
Oomi G and Woods S B 1985 *Phys. Status Solidi* b **130** K71
Overhauser A W 1984 *Phys. Rev. Lett.* **53** 64
Pettifor D G 1977 *J. Phys. F: Met. Phys.* **7** 613
Skriver H L 1983 *The LMTO Method* (Berlin: Springer)
—— 1985 *Phys. Rev.* B **31** 1909
Smith H G 1987 *Phys. Rev. Lett.* **58** 1228
Sukhoparov V A and Telepnev A S 1980 *Prib. Tekhn. Exp. (Sov. Phys.–PTE)* **5** 204–5
Vaks V G, Kravchuk S P and Trefilov A V 1977a *Fiz. Tverd. Tela* **19** 1271
—— 1977b *Fiz. Tverd. Tela* **19** 3396
—— 1977c *Fiz. Met. Metallov.* **44** 1151
Vaks V G and Trefilov V A 1988 *J. Phys. F: Met. Phys.* **18** 213
Vaks V G, Zarochentsev E V, Kravchuk S P and Safronov V P 1978 *J. Phys. F: Met. Phys.* **8** 725
Vindryaevsky B A, Chernyshov A A and Sukhoparov V A 1980 *Prib. Tekhn. Exp. (Sov. Phys.–PTE)* **4** 225–7
Vindryaevsky B A, Ishmaev S N, Sadikov I P and Chernyshov A A 1981 *Nucl. Instrum. Methods* **180** 79
Voronov F F, Gromnitskaya E L and Stalgorova O V 1987 *Fiz. Met. Metallov.* **64** 1084
Voronov F F and Stalgorova O V 1973 *Fiz. Tverd. Tela* **20** 452
Wilson J A and de Podesta M 1986 *J. Phys. F: Met. Phys.* **16** L121
Xu J H, Oguchi T and Freeman A J 1987 *Phys. Rev.* B **35** 6940
Young D A and Ross M 1984 *Phys. Rev.* B **29** 682
Zdetsis A D 1986 *Phys. Rev.* B **34** 7666
Zener C 1947 *Phys. Rev.* **71** 846